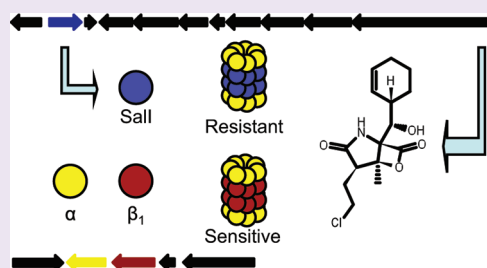


# Bacterial Self-Resistance to the Natural Proteasome Inhibitor Salinosporamide A

Andrew J. Kale,<sup>†</sup> Ryan P. McGlinchey,<sup>†</sup> Anna Lechner,<sup>†</sup> and Bradley S. Moore<sup>†,‡,\*</sup><sup>†</sup>Center for Marine Biotechnology and Biomedicine, Scripps Institution of Oceanography<sup>‡</sup>Skaggs School of Pharmacy and Pharmaceutical Sciences, University of California at San Diego, 9500 Gilman Drive, La Jolla, California 92093, United States

Supporting Information

**ABSTRACT:** Proteasome inhibitors have recently emerged as a therapeutic strategy in cancer chemotherapy, but susceptibility to drug resistance limits their efficacy. The marine actinobacterium *Salinispora tropica* produces salinosporamide A (NPI-0052, marizomib), a potent proteasome inhibitor and promising clinical agent in the treatment of multiple myeloma. Actinobacteria also possess 20S proteasome machinery, raising the question of self-resistance. We identified a redundant proteasome  $\beta$ -subunit, Sall, encoded within the salinosporamide biosynthetic gene cluster and biochemically characterized the Sall proteasome complex. The Sall  $\beta$ -subunit has an altered substrate specificity profile, 30-fold resistance to salinosporamide A, and cross-resistance to the FDA-approved proteasome inhibitor bortezomib. An A49V mutation in Sall correlates to clinical bortezomib resistance from a human proteasome  $\beta$ 5-subunit A49T mutation, suggesting that intrinsic resistance to natural proteasome inhibitors may predict clinical outcomes.



The 26S proteasome is a macromolecular enzymatic complex responsible for the regulated hydrolysis of cellular proteins that in turn mediates processes such as amino acid recycling, cell cycle control, cell differentiation, and apoptosis.<sup>1</sup> Ubiquitinated proteins are targeted by the 19S regulatory cap and transferred into the interior of the cylindrical 20S proteasome core particle for degradation by catalytic  $\beta$ -subunits having nucleophilic N-terminal threonine residues.<sup>1</sup> Eukaryotes harbor a 2-fold symmetrical  $\alpha_{(1-7)}\beta_{(1-7)}\beta_{(1-7)}\alpha_{(1-7)}$  barrel-shaped 20S structure with three active  $\beta$ -subunits ( $\beta$ 1, caspase-like (C-L);  $\beta$ 2, trypsin-like (T-L); and  $\beta$ 5, chymotrypsin-like (CT-L)) that display distinct proteolytic specificities.<sup>2</sup> Their catalytic inhibition with mechanism-based small molecules has exposed the proteasome as an important therapeutic target in cancer and inflammation.<sup>3</sup> Recently the dipeptide boronic acid bortezomib (1, Figure 1) was approved by the FDA for the treatment of relapsed multiple myeloma and mantle cell lymphoma as a first in class proteasome inhibitor (PI) that functions as a reversible inhibitor of the  $\beta$ 5-subunit.<sup>4,5</sup> Acquired resistance to bortezomib, however, has already emerged and limits its pronounced clinical benefit that in part is due to point mutations in the proteasome  $\beta$ 5-subunit.<sup>6-9</sup>

Salinosporamide A (2), a potent PI naturally synthesized by the marine bacterium *Salinispora tropica*, represents an alternative treatment option due to its distinct chemical structure and mechanism of action.<sup>10</sup> Its biosynthesis in an actinobacterium, which is unique among bacterial divisions to maintain a 20S proteasome,<sup>1</sup> with a simplified  $\alpha_7\beta_7\beta_7\alpha_7$  structure, raises the question of the molecular basis behind natural proteasome resistance and whether this mechanism correlates to clinical drug

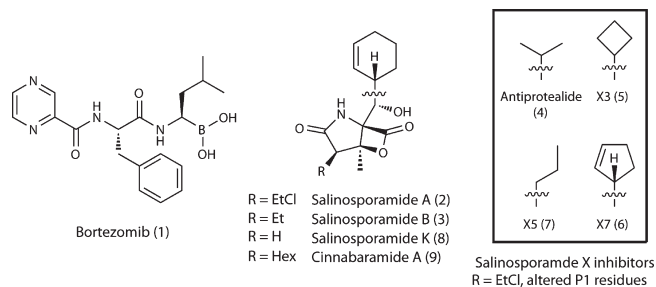


**Figure 1.** Chemical structures of small molecule 20S PIs tested in this study. The respective P1 residues (Leu in bortezomib; cyclohexenyl in salinosporamides A, B, K, and cinnabaramide A; and the boxed residues in the salinosporamide X series) interact with the S1 specificity pocket of the proteasome  $\beta$ -subunit upon binding. The displaceable chloride of salinosporamide A confers irreversible inhibition.

resistance. Unlike the eukaryotic 26S proteasome that is essential for survival,<sup>11</sup> the 20S proteasome has been inactivated in several actinobacteria without loss of viability.<sup>12,13</sup> *Mycobacterium tuberculosis* is a notable exception that requires the proteasome for pathogenicity in response to host-induced oxidative stress.<sup>14</sup> The recent discovery of the prokaryotic ubiquitin-like protein (PUP) has established that the actinobacterial proteasome regulates the

Received: July 21, 2011

Accepted: September 1, 2011

Published: September 01, 2011

controlled destruction of targeted proteins.<sup>15–18</sup> Elucidating the specific proteins and pathways regulated by the 20S proteasome in actinobacteria remains an active area of investigation.

Salinosporamide A belongs to a growing family of potent natural PIs that also includes the actinomycete natural products lactacystin, cinnabaramide A, epoxomicin, and belactosine A.<sup>10,19</sup> However, despite the many examples of natural product PIs being produced by microbes that must maintain their own functional proteasomes, the biochemical basis for natural resistance has not been defined. We describe here the identification and characterization of a 20S proteasome target modification resistance mechanism to salinosporamide A in the producing organism *S. tropica*.

## RESULTS AND DISCUSSION

**Identification of a Transcriptionally Active 20S Proteasome  $\beta$ -Subunit in the Salinosporamide Biosynthetic Gene Cluster.** We recently sequenced the complete genome of *S. tropica* CNB-440 and functionally characterized the salinosporamide A gene locus.<sup>20,21</sup> Curiously, toward one end of the 41-kb *sal* gene cluster resides the gene *salI* (Strop\_1015) encoding a proteasome  $\beta$ -subunit. Its physical location in a biosynthetic operon associated with a PI strongly suggested its involvement in resistance through target modification, a strategy more commonly associated with antibiotic resistance.<sup>22</sup> Further genomic analysis of *S. tropica* CNB-440 identified a typical actinobacterial 20S proteasome gene cluster (Strop\_2241–2247) that includes adjacent genes encoding  $\alpha$  and  $\beta$  proteasome subunits. We reasoned that the SalI  $\beta$ -subunit would additionally complex with the lone  $\alpha$ -subunit during the biosynthesis of salinosporamide A to render a functional 20S proteasome with greater tolerance to the PI. To this end, we analyzed mRNA transcripts of *Strop\_2245* ( $\alpha$ -subunit), *Strop\_2244* ( $\beta$ -subunit), *salI*, and the salinosporamide biosynthesis gene *salL* as a reference to correlate SalI to inhibitor production. We observed active transcription of *salI* in parallel to the proteasome  $\alpha$  and  $\beta$  subunits and *salL* (Figure 2a), suggesting that SalI has the potential to form an active proteasome complex during salinosporamide A biosynthesis.

**In Vitro Characterization of *S. tropica* Proteasome Complexes.** To generate homogeneous proteasome complexes for *in vitro* analysis, we heterologously expressed proteasome subunits in *Escherichia coli*, which lacks an endogenous 20S proteasome. Individually expressed Strop\_2244  $\beta$ -subunit (referred to henceforth as  $\beta_1$ ) and SalI remained insoluble until complexed with the  $\alpha$ -subunit, suggesting a mutual dependence for correct folding. Coexpression of the readily soluble  $\alpha$ -subunit as an N-terminal His<sub>6</sub>-tagged protein (29.1 kDa) with untagged  $\beta_1$  or SalI (23.4 and 24.6 kDa, respectively, after prosequence removal) and purification of the respective complexes by Ni<sup>2+</sup> affinity chromatography and size-exclusion chromatography gave protein bands in excess of 669 kDa (Figure 2b), which was consistent with fully assembled  $\alpha_7(\beta_1)_7(\beta_1)_7\alpha_7$  (ca. 735 kDa) and  $\alpha_7\text{SalI}_7\alpha_7$  (ca. 752 kDa) proteasome complexes. Proteolytic activity of these bands was verified by the application of a fluorogenic peptide-7-amino-4-methylcoumarin (amc) substrate directly to the gel (Figure 2c). We next explored the respective hydrolytic activities and substrate specificities of the purified proteasome complexes using an array of peptide-amc substrates (Table 1). The  $\alpha/\beta_1$  complex was most active against the T-L substrate Ac-RLR-amc with further activity against the CT-L substrate Suc-LLVY-amc and the general substrate Z-VKM-amc. For the  $\alpha/\text{SalI}$  complex, T-L activity was abolished while that of

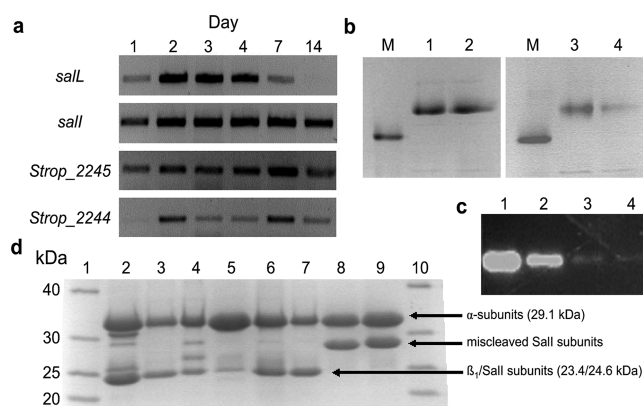


**Figure 2.** Gel-based analysis of proteasomal transcription, heterologous expression, and subunit assembly. (a) Proteasome transcriptional analysis in *S. tropica*. mRNA was isolated at multiple time points, and transcripts of *salI*, *Strop\_2245* ( $\alpha$ -subunit), *Strop\_2244* ( $\beta_1$ -subunit), and the salinosporamide chlorinase *salL* are shown. The *salI* gene is actively transcribed at all time points that salinosporamide A is being produced, as indicated by transcription of *salL*. Concurrent transcription of the  $\alpha$ -subunit indicates that the  $\alpha/\text{SalI}$  complex may form *in vivo* with salinosporamide production. (b) Native PAGE analysis of the assembled proteasome complexes. Lanes: M, thyroglobulin (669 kDa); 1,  $\alpha/\beta_1$ ; 2,  $\alpha/\beta_1$  preincubated with 75  $\mu\text{M}$  salinosporamide A; 3,  $\alpha/\text{SalI}$ ; and 4,  $\alpha/\text{SalI}$  preincubated with 75  $\mu\text{M}$  salinosporamide A. Major bands above the 669 kDa marker correspond to fully assembled proteasomes. (c) Fully assembled proteasome bands, based on migration of and with the same lane assignments as panel b, were visualized in overlay assays using the fluorogenic substrate Suc-LLVY-amc. (d) Denaturing 16% SDS-PAGE analysis of the proteasome complexes. Lanes: 1, 10, NativeMark ladder; 2,  $\alpha/\beta_1$ ; 3,  $\alpha/\beta_1$  M45F; 4,  $\alpha/\beta_1$  A49V; 5,  $\alpha/\beta_1$  M45F/A49V; 6,  $\alpha/\text{SalI}$ ; 7,  $\alpha/\text{SalI}$  F45M; 8,  $\alpha/\text{SalI}$  V49A; and 9,  $\alpha/\text{SalI}$  F45M/V49A. The increased size of SalI in lanes 8 and 9 indicate improper prosequence cleavage due to the V49A mutation.

**Table 1.** Hydrolysis Rates of *S. tropica* Proteasome Complexes for All Active Substrates<sup>a</sup>

proteasome complex	hydrolysis rate (nmol h <sup>-1</sup> mg <sup>-1</sup> )		
	Suc-LLVY-amc	Ac-RLR-amc	Z-VKM-amc
$\alpha/\beta_1$	56.0 ± 1.3	93.8 ± 5.0	51.6 ± 2.7
$\alpha/\beta_1$ M45F	46.9 ± 10.7	89.4 ± 6.6	53.8 ± 1.9
$\alpha/\beta_1$ A49V	inactive	inactive	ND <sup>b</sup>
$\alpha/\beta_1$ M45F/A49V	inactive	inactive	ND <sup>b</sup>
$\alpha/\text{SalI}$	3.4 ± 0.2	inactive	19.4 ± 0.6
$\alpha/\text{SalI}$ F45M	33.1 ± 2.5	inactive	78.4 ± 0.3
$\alpha/\text{SalI}$ V49A	inactive	inactive	inactive
$\alpha/\text{SalI}$ F45M/V49A	inactive	inactive	inactive

<sup>a</sup> No activity was observed with substrates Z-LLL-amc, MeOSuc-AAPV-amc, Z-LLE-amc, and Suc-APA-amc. Data shown is the mean ± standard deviation,  $N = 3$ . <sup>b</sup> Both  $\alpha/\beta_1$  A49V and  $\alpha/\beta_1$  M45F/A49V displayed detectable activity toward substrate Z-VKM-amc. However, these complexes were recovered in low yield and were prone to aggregation upon purification, and therefore hydrolytic rates were not determined (ND).

CT-L was highly reduced. Instead, the  $\alpha/\text{SalI}$  complex was 6-fold more active against Z-VKM-amc than with CT-L substrate Suc-LLVY-amc, which is often preferred by other actinobacterial proteasomes.<sup>23–26</sup> We thus observed a markedly different substrate specificity between the two complexes in which the  $\alpha/\text{SalI}$

**Table 2. Salinosporamide A Inhibition ( $IC_{50}$ ) Values for All Wild-Type and Mutant Complexes**

proteasome complex	substrate <sup>a</sup>	$IC_{50}$ ( $\mu M$ ) salinosporamide A
$\alpha/\beta_1$	LLVY	$3.1 \pm 0.2$
	RLR	$1.7 \pm 0.8$
	VKM	$1.2 \pm 0.1$
$\alpha/\beta_1$ M45F	VKM	$1.2 \pm 0.1$
	$\alpha/\beta_1$ A49V	$13.6 \pm 2.2$
$\alpha/\beta_1$ M45F/A49V	VKM	$15.3 \pm 2.2$
	$\alpha/SalI$	LLVY
RLR		inactive
VKM		$36.8 \pm 2.4$
$\alpha/SalI$ F45M	VKM	$45.5 \pm 2.3$
	$\alpha/SalI$ V49A	inactive
$\alpha/SalI$ F45M/V49A	VKM	inactive

<sup>a</sup> Substrate represents amino acid residues preceding fluorescent amc tag (e.g., LLVY = Suc-LLVY-amc). Data shown is the mean  $\pm$  standard deviation,  $N = 3$ .

**Table 3. Inhibition ( $IC_{50}$ ) Values of Wild-Type  $\alpha/\beta_1$  and  $\alpha/SalI$  Proteasome Complexes with Various Peptide-Based Inhibitors<sup>a</sup>**

inhibitor	$\alpha/\beta_1$ $IC_{50}$ ( $\mu M$ )	$\alpha/SalI$ $IC_{50}$ ( $\mu M$ )
Salinosporamide A	$1.2 \pm 0.1$	$36.8 \pm 2.4$
Salinosporamide B	$19.2 \pm 3.5$	$138.7 \pm 27.3$
Bortezomib	$3.3 \pm 0.2$	$42.7 \pm 3.4$
Antiprotealide	$103.6 \pm 7.2$	>250
Salinosporamide X3	>250	>250
Salinosporamide X5	>250	>250
Salinosporamide X7	$3.6 \pm 0.2$	>250

<sup>a</sup> All assays were performed using the Z-VKM-amc substrate. Inhibitor insolubility prevented accurate  $IC_{50}$  determination at concentrations exceeding  $250 \mu M$ . Data shown is the mean  $\pm$  standard deviation,  $N = 3$ .

complex was approximately 5-fold less active than the  $\alpha/\beta_1$  complex with the substrates evaluated.

We next interrogated the  $\alpha/\beta_1$  and  $\alpha/SalI$  complexes against salinosporamide A inhibition to explore their relevant tolerance. As hypothesized, we observed a 16- to 30-fold increase in  $IC_{50}$  with the  $\alpha/SalI$  complex in comparison to the  $\alpha/\beta_1$  complex (Table 2). Both proteasome complexes exhibited time-dependent inhibition by salinosporamide A (Supplementary Figure 1) and no recovery of proteolytic activity was observed after buffer exchange to remove salinosporamide A. The resistance of the  $\alpha/SalI$  complex to inhibition was conserved with the reversibly inhibiting deschloro analog salinosporamide B (3)<sup>27</sup> and the structurally distinct bortezomib, showing 7- and 13-fold increases in  $IC_{50}$  values, respectively (Table 3). The resistance to both salinosporamide A and bortezomib, combined with the marked shift in proteolytic specificities, indicated that  $\beta_1$  and SalI have significant differences in substrate binding pocket dynamics.

**Probing Proteasome Binding Pocket Residues with Mutational Analysis.** To gain insight into the molecular basis governing SalI's PI resistance, we scrutinized its amino acid residues lining the conserved S1 and S2 pockets since the compact nature of salinosporamide restricts its proteasome binding interactions to these sites. Crystallographic analysis of salinosporamide A

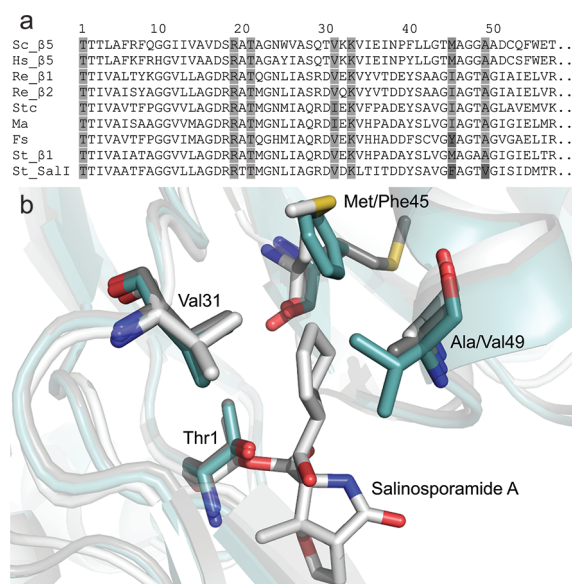


**Figure 3.** Comparison of actinobacterial and eukaryotic  $\beta$ -subunit S1 binding pocket residues. (a) A partial sequence alignment of characterized actinomycete  $\beta$ -subunits and the CT-L  $\beta_5$ -subunits of *Saccharomyces cerevisiae* (Sc) and *Homo sapiens* (Hs) is shown from Thr1 to position 57. The actinobacterial  $\beta$ -subunits of *Rhodococcus erythropolis* PR4 (Re), *Streptomyces coelicolor* A3(2) (Stc), *Micromonospora aurantiaca* ATCC 27029 (Ma), *Frankia* sp. ACN14a (Fs), and *Salinispora tropica* CNB-440 (St) are displayed. Residues previously shown to interact with salinosporamide A during binding to the  $\beta_5$ -subunit of *S. cerevisiae* are highlighted. Darker shades of gray indicate deviation from the consensus sequence. A full alignment is shown in Supplementary Figure 2. (b) A structural depiction of salinosporamide A bound to the 20S proteasome. Residues forming the S1 binding pocket are shown. The Sc  $\beta_5$ -subunit with salinosporamide A bound (white, PDB 2FAK chain K) is overlaid with  $\beta_1$  (gray) and SalI (blue) of St, both homology modeled against the prokaryotic proteasome  $\beta$ -subunit of Re (PDB 1QSQ chain H). The substitution of Phe45 and Val49 in SalI were predicted to alter substrate and inhibitor binding and therefore targeted for mutagenesis.

bound to the  $\beta_5$ -subunit of the *Saccharomyces cerevisiae* proteasome previously revealed beneficial hydrophobic interactions between its cyclohexenyl side chain and several residues of the S1 binding pocket, most notably Met45, yet minimal contact with the S2 pocket.<sup>27</sup> Alignment of  $\beta_1$ , SalI,  $\beta_5$  from *S. cerevisiae* and *Homo sapiens*, and previously characterized actinobacterial proteasome  $\beta$ -subunits revealed that SalI possesses unique Phe45 and Val49 residues, both located within the S1 binding pocket (Figure 3a). Position 45 forms the base of the S1 binding pocket and is known to confer CT-L, T-L, or C-L preference to the eukaryotic  $\beta$ -subunits, while position 49 resides at the entrance of the pocket (Figure 3b).<sup>2</sup> We thus targeted both positions by site-directed mutagenesis and generated mutants in which we exchanged their residues in order to investigate substrate specificity and salinosporamide resistance in both *S. tropica*  $\beta$ -subunits,  $\beta_1$  and SalI.

Mutagenesis of the  $\beta_1$  Met45 residue, which is conserved in the *S. cerevisiae* and human  $\beta_5$ -subunits where it contributes to their CT-L activities, to Phe as in SalI resulted in the  $\alpha/\beta_1$  M45F mutant that maintained its native proteolytic activity (Table 1) and sensitivity to salinosporamide A (Table 2). Conversely, the  $\alpha/SalI$  F45M mutant had significantly greater hydrolytic activity for its substrates Suc-LLVY-amc and Z-VKM-amc at  $\sim 10$  and 4 times, respectively, its native activity (Table 1). This mutant did

not engender new activity against the five previously tested inactive substrates, revealing that substrate specificity was not altered as originally envisaged, just its catalytic efficiency. Further,  $\alpha$ /SalI F45M was slightly more resistant to salinosporamide A than the native  $\alpha$ /SalI complex (Table 2), indicating that position 45 is not a major determinant in salinosporamide A resistance.

We rather hypothesized that position 49 contributes to salinosporamide resistance as the substitution of the larger Val residue in SalI for the conserved Ala residue that typifies  $\beta$ -subunits would constrict the S1 binding pocket and hinder inhibitor binding. Previously an A49V mutation was identified in the *S. cerevisiae*  $\beta$ 5-subunit that resulted in a shift of substrate specificity away from CT-L activity.<sup>28</sup> Similar A49T acquired mutations in human monocytic/macrophage, multiple myeloma, and lymphoblastic Jurkat T cell lines were recently shown to confer resistance to bortezomib and cross-resistance to other peptide-based PIs.<sup>7–9</sup> We thus first generated the  $\alpha/\beta_1$  A49V mutant. This mutant lost most of its hydrolytic activity while maintaining Z-VKM-amc activity, albeit at reduced levels (Table 1). When incubated with salinosporamide A, we observed greater than a 10-fold increase in its IC<sub>50</sub> (Table 2). Unfortunately, our attempts to further correlate the role of Val49 in salinosporamide resistance with  $\alpha$ /SalI V49A were unsuccessful since this mutant complex lost its hydrolytic activity. Denaturing PAGE revealed a 2–3 kDa increase in the SalI subunits containing the V49A mutation, indicating activity was lost due to improper prosequence cleavage (Figure 2d). The  $\alpha/\beta_1$  M45F/A49V and  $\alpha$ /SalI F45M/V49A double mutants behaved similarly to the respective position 49 single mutants, indicating that this residue is significantly more influential to S1 binding pocket dynamics in both complexes.

The mechanism of self-resistance to endogenously produced salinosporamide A in *S. tropica* appears to have independently evolved in human cancer cell lines with prolonged exposure to the drug. Intriguingly, acquired human resistance to a natural anticancer agent that mirrors the evolved natural resistance strategy was also recently described for the topoisomerase I inhibitor camptothecin. In this case, the camptothecin-containing medicinal plant carries a point mutation in the encoding topoisomerase I gene that is identical to one found in resistant human cell lines.<sup>29</sup> However, there is a subtle difference in the salinosporamide and camptothecin resistance examples since camptothecin is produced by an endophytic fungus associated with the plant,<sup>30</sup> and thus genes for biosynthesis and resistance are rather decoupled between the producer and the resistant host.

**Targeting SalI for Inhibition with Modified P1 Residues.** Mutational analysis revealed the SalI A49V mutation to be the primary driver of salinosporamide A resistance. The observed cross-resistance to bortezomib, bearing a P1 leucine residue, and decreased activity with the CT-L substrate suggested that Val49 diminishes the potent inhibition of salinosporamide A via S1 binding pocket constriction. To probe this premise, we further interrogated the *S. tropica* 20S proteasome complexes with salinosporamide derivatives bearing modified C-5 residues corresponding to the P1 site. We thus assayed four salinosporamide X derivatives previously generated by mutasynthesis<sup>31</sup> in which the cyclohexenyl ring of salinosporamide A was replaced with smaller (antiprotealide (4), salinosporamides X3 (5) and X7 (6)) or more flexible (salinosporamide X5 (7)) aliphatic P1 residues. In each case, we measured a loss in proteasome inhibition in relation to salinosporamide A (Table 3), suggesting a more complicated picture in inhibitor binding and S1 pocket dynamics.

**Survey of Secondary Proteasomal  $\beta$ -Subunits in Actinomycetes.** Having validated the relationship between the endogenous *S. tropica* PI salinosporamide and the resistance proteasome  $\beta$ -subunit SalI, we next probed other actinobacterial genomes for similar associations in order to query whether this is a common phenomenon for PI biosynthesis. Since salinosporamide A is structurally related to the PIs salinosporamide K (8) from “*Salinispora pacifica*” strain CNT-133A<sup>32</sup> and the cinnabaramides (9) from *Streptomyces* sp. JS360,<sup>33</sup> we first probed their biosynthetic loci. We cloned and partially sequenced the cinnabaramide biosynthetic gene cluster and identified an associated *salI* homologue (46% sequence identity) whose product has the resistance Phe45/Val49 sequence signature (Table 4). The complete cinnabaramide biosynthetic cluster, including this 20S proteasome  $\beta$ -subunit (CinJ), has been independently published.<sup>34</sup> As in the case with *S. tropica*, *Streptomyces* sp. JS360 also harbors a primary 20S proteasome gene cluster that includes a  $\beta$ -subunit containing residues Ile45 and Ala49, which is consistent with previously characterized actinobacterial  $\beta$ -subunits.<sup>23–26</sup> Sequence analysis of the recently sequenced “*S. pacifica*” salinosporamide K biosynthetic gene cluster, on the other hand, did not reveal an associated proteasome  $\beta$ -subunit, which may correlate with salinosporamide K’s lower biosynthetic titer and diminished inhibitory activity.<sup>32</sup>

BLAST analysis of the *S. tropica*  $\beta_1$ -subunit against all available actinobacterial genomes uncovered several organisms with dual proteasome  $\beta$ -subunits. Comparison of the primary and secondary proteasome  $\beta$ -subunits of *Streptomyces avermitilis* MA-4680, *Thermomonospora curvata* DSM 43183, and *Streptomyces bingchenggensis* BCW-1 showed that Ala49 is switched to either Val or Leu in one of the two subunits (Table 4). In two cases, Val49 occurs in the freestanding secondary  $\beta$ -subunit, as is the case with *S. tropica*, while the primary  $\beta$ -subunit of *S. bingchenggensis* contains Leu49. Further sequence analysis of the gene neighborhoods of the secondary proteasome  $\beta$ -subunits revealed in the case of *S. bingchenggensis* a hybrid nonribosomal peptide synthetase–polyketide synthase biosynthetic gene cluster (ADI05330/ADI05329) located immediately adjacent to its secondary  $\beta$ -subunit. This gene cluster is predicted to encode the biosynthesis of a tripeptide natural product with a modified C-terminal acetate extension. As many synthetic and natural PIs are short peptides with an electrophilic modification at the C-terminus,<sup>19</sup> we anticipate that this cluster encodes an orphan PI with a novel peptidic structure. This clear association of a secondary proteasome  $\beta$ -subunit with a natural product biosynthetic gene cluster may signal a new experimental paradigm for the discovery of natural PIs.

**Conclusions.** The recruitment of a pathway-specific proteasome  $\beta$ -subunit to assemble with the primary  $\alpha$ -subunit to form a 20S proteasome complex ( $\alpha$ /SalI) that is both hydrolytically active and relatively resistant to PIs is unprecedented and defines a new mechanism of natural product resistance. This evolved resistance mechanism in a PI-producing microbe is strikingly similar to the analogous target modification paradigm recently reported for bortezomib treatment in human cancer cell lines, thereby suggesting that natural PI chemotherapy, which includes salinosporamide A, may ultimately be similarly susceptible to acquired resistance by proteasome modification.

## METHODS

**Materials.** Salinosporamides A and B were purified from cultures of *S. tropica* CNB-440.<sup>35</sup> Proteasome inhibitors of the salinosporamide X series were produced and purified from a genetically modified *S. tropica*

Table 4. Sequence Comparison of Secondary  $\beta$ -Subunits in Actinomycetes<sup>a</sup>

organism	$\beta$ -subunit <sup>b</sup>	accession no.	motif 45–49	% identity <sup>c</sup>	E-value <sup>d</sup>
<i>Salinispora tropica</i> CNB-440	1°, $\beta_1$	YP_001159072	MAGAA	58	NA
	2°, SallI	YP_001157868	FAGTV	100	$6.0 \times 10^{-68}$
<i>Streptomyces</i> sp. JS360	1°	JF970179	IAGTA	52	$5.0 \times 10^{-75}$
	2°, CinJ	JF970180	FAGSV	46	$3.0 \times 10^{-71}$
<i>Streptomyces avermitilis</i> MA-4680	1°	NP_827857	IAGTA	53	$7.0 \times 10^{-77}$
	2°	NP_823988	FAGTV	51	$6.0 \times 10^{-66}$
<i>Thermomonospora curvata</i> DSM 43183	1°	YP_003299915	IAGTA	56	$2.0 \times 10^{-76}$
	2°	YP_003300043	MAGTV	50	$3.0 \times 10^{-61}$
<i>Streptomyces bingchengensis</i> BCW-1	1°	ADI11600	IAGTL	52	$9.0 \times 10^{-75}$
	2°	ADI05332	IAGTA	52	$9.0 \times 10^{-65}$

<sup>a</sup>The two previously characterized  $\beta$ -subunits of *R. erythropolis* were omitted as both associate with  $\alpha$ -subunits.<sup>25</sup> The full sequence alignment is provided in Supplementary Figure 2. <sup>b</sup>The designation of 1° is based on  $\beta$ -subunit association with a proteasomal gene cluster containing an  $\alpha$ -subunit and accessory proteins, whereas 2°  $\beta$ -subunits are found without other proteasomal encoding genes and often cluster with natural product biosynthesis genes. <sup>c</sup>Relative to SallI without prosequence. <sup>d</sup>Relative to *S. tropica*  $\beta_1$  without prosequence.

strain as previously described.<sup>31,36</sup> All chemicals purchased were of the highest quality. Proteasome inhibitor Velcade (Bortezomib) was purchased from LC Laboratories, and the seven 7-amino-4-methylcoumarin (amc) tagged peptide substrates were purchased as follows: substrates Z-Val-Lys-Met-amc, Z-Leu-Leu-Leu-amc, Suc-Leu-Leu-Val-Tyr-amc, MeOSuc-Ala-Ala-Pro-Val-amc, Ac-Arg-Leu-Arg-amc, and Z-Leu-Leu-Glu-amc from Enzo Life Sciences and substrate Suc-Ala-Pro-Ala-amc from Peptides International, Inc.

**mRNA Transcript Analysis.** Total RNA was extracted from *S. tropica* CNB-440 and converted to cDNA as reported previously.<sup>21</sup> PCR was run for 25 cycles using Taq polymerase (New England Biolabs) and 500 ng of cDNA in 10  $\mu$ L reactions. Primers used were *sallI*, forward 5' TCGTGGACATAACCCATGAC 3' and reverse 5' AGGACCTCGT-GACTCGAC 3'; *sallI*, forward 5' TAGTCGTCCGTGATCGTGAG 3' and reverse 5' GCCGTCCACGTTCTTAACAT 3'; *Strop\_2244*, forward 5' CTGGAGACTACGAGAAGAC 3' and reverse 5' GTC-ACGTCGAAGCTGAAG 3'; and *Strop\_2245*, forward 5' CCTGAAC-GGTCTGAGCTAC 3' and reverse 5' GGTACAGTTCGTCGTCCTC 3'. PCR products were approximately 250 bp in size.

**Plasmid Construction.** Proteasome  $\alpha$  (*Strop\_2245*, accession: YP\_001159073) and  $\beta_1$  (*Strop\_2244*, accession: YP\_001159072) or SallI (*Strop\_1015*, accession: YP\_001157868) subunits were sequentially cloned from genomic DNA of *S. tropica* CNB-440 into the ampicillin-resistant pETDuet-1 coexpression vector (EMD Chemicals) to generate  $\alpha/\beta_1$  pETDuet and  $\alpha$ /SallI pETDuet. The  $\alpha$ -subunit contained an N-terminal His<sub>6</sub> tag while the  $\beta_1$  and SallI subunits were untagged. An additional  $\beta_1$ -subunit was cloned into the kanamycin resistant pHis8 expression vector.<sup>37</sup> PCR reactions used *Pfu* Turbo DNA polymerase and were sequenced by Seqxcel, Inc.

The  $\beta_1$ -subunit was amplified for the pHis8 vector with the primers forward 5' CCCATGGCGGATCCGTGGCAGCGGCTTTCGACC 3' and reverse 5' CCCATGGCGAATTCTCAGCCGCCCGGATTCTCC 3'. The  $\alpha$ -subunit was amplified for MCS1 of pETDuet-1 with the primers forward 5' CACAGCCAGGATCCGGTGGCCATGCAGTTCTACGCC 3' and reverse 5' CCCATGGCGAATTCCTAGGGGGCCTCGGAA-TCGG 3'.  $\beta_1$  was amplified for MCS2 of pETDuet-1 with the primers forward 5' GAGATATACATATGGCAGCGGCTTTCGACCCATC 3' and reverse 5' CCCATGGCGATATCTCAGCCGCCCGGATTCTCC 3'.

SallI was amplified for MCS2 of pETDuet-1 with the primers forward 5' GAGATATACATATGAATCGGGGTCTGCCGTCCAC 3' and reverse 5' CCCATGGCGATATCTCAGGACGCGGTAAGCTTCG 3'. The introduced *Bam*HI, *Eco*RI, *Nde*I and *Eco*RV sites are underlined. The start and stop codons are shown in bold.

**Site-Directed Mutagenesis.** Site-directed mutagenesis was performed using the Stratagene Quikchange kit (Agilent Technologies). Single point mutations were performed using the  $\alpha/\beta_1$  pETDuet and  $\alpha$ /SallI pETDuet constructs as templates to generate  $\alpha/\beta_1$  M45F pETDuet,  $\alpha/\beta_1$  A49V pETDuet,  $\alpha$ /SallI F45M pETDuet, and  $\alpha$ /SallI V49A pETDuet. Positions 45 and 49 refer to the amino acid position of the  $\beta_1$  or SallI subunit from Thr1 after prosequence cleavage. Double mutations were performed sequentially. The  $\alpha/\beta_1$  M45F pETDuet plasmid was used as a template to generate the  $\alpha/\beta_1$  M45F/A49V double mutant while the  $\alpha$ /SallI F45M pETDuet plasmid was similarly used to generate the  $\alpha$ /SallI F45M/V49A double mutant. Both subunits of the mutant vectors were resequenced for verification following mutagenesis.

Primers sequences used were as follows with mutation sites underlined:  $\alpha/\beta_1$  M45F forward 5' CTCCCTGGTGGGCTTCGCGGGT-GCCGCC 3' and reverse 5' GGCGGCACCCGCGAAGCCACCA-GGGAG 3';  $\alpha/\beta_1$  A49V forward 5' CATGGCGGGTGCCTCG-GAATCGGGATC 3' and reverse 5' GATCCCATTCCGACGGCA-CCC GCCATG 3';  $\alpha/\beta_1$  M45F/V49A (from  $\alpha/\beta_1$  M45F) forward 5' CTTCGCGGGTCCCGTCCGAATCGGGATC 3' reverse 5' GATC-CCGATTCGACGGCACCCGCGAAG 3';  $\alpha$ /SallI F45M forward 5' CTATTCGGCGGTGGTATGGCCGGCACGGTGGGC 3' and reverse 5' GCCCACCGTGCCGGCCATACCCAGCCCGAATAG 3';  $\alpha$ /SallI V49A forward 5' GTTTCGCCGGCACGGCAGGCATCTC-CATTGAC 3' and reverse 5' GTCAATGGAGATGCCGTGCCGTG-CCGGCGAAAC 3';  $\alpha$ /SallI F45M/V49A (from  $\alpha$ /SallI F45M) forward 5' GTATGGCCGGCACGGCAGGCATCTCCATTGAC 3' and reverse 5' GTCAATGGAGATGCCGTGCCGTGCCGCCATAC 3'.

**Protein Expression.** All expression vectors were transformed into *Escherichia coli* BL21 (DE3). To increase titers of the  $\alpha/\beta_1$  wild-type complex, a second  $\beta_1$  expression plasmid,  $\beta_1$  pHis8, was transformed concurrently with  $\alpha/\beta_1$  pETDuet. A 10 mL culture in LB broth containing 100  $\mu$ g mL<sup>-1</sup> ampicillin was grown overnight at 37 °C. This was used to inoculate a 1 L culture of ZY media with autoinduction containing 100  $\mu$ g mL<sup>-1</sup> ampicillin.<sup>38</sup> In the case of the wild-type  $\alpha/\beta_1$  proteasome expression, 50  $\mu$ g mL<sup>-1</sup> kanamycin was also added to starter and expression cultures. Expression cultures were grown on an orbital shaker for 20 h at 28 °C.

**Protein Purification.** All protein purification steps took place at 4 °C. Protein purification buffers contained 300 mM NaCl, 50 mM sodium phosphate adjusted to pH 8.0, and increasing concentrations of imidazole. Buffers A (lysis), B (wash), and C (elution) contained 10, 20, and 250 mM imidazole, respectively. Cells were pelleted at 6,300g for 15 min, resuspended in buffer A, and lysed with six 30 s bursts of probe sonication with resting periods of 30 s. The lysate was centrifuged for

45 min at 20,000g. Soluble protein was collected and equilibrated with Ni-NTA resin for 1 h before it was purified by Ni-NTA affinity chromatography, washed with several volumes of buffer B and eluted with 10 mL of buffer C. Washed and eluted protein was concentrated with a Vivaspin 100 kDa cutoff spin concentrator (GE biosciences) and resuspended in 100 mM Tris-HCl at pH 8.0. Concentrated protein was further purified by size exclusion chromatography on a HiLoad 16/60 Superdex 200 column (GE biosciences) with a 100 mM Tris-HCl pH 8.0 mobile phase and reconcentrated with a vivaspin 100 kDa cutoff protein concentrator.

**Native Gel Analysis and Fluorescent Overlay Assay.** A 10  $\mu$ g sample of  $\alpha/\beta_1$  or  $\alpha/\text{SalI}$  was loaded onto an Invitrogen (4–16%) NativePAGE gel (Life Technologies). The gel was run at 150 V at 4 °C. For direct band visualization, the gels were washed and stained with Coomassie Brilliant Blue. For fluorescent visualization assays, the unstained native gel was briefly washed with H<sub>2</sub>O and then submerged in 25  $\mu$ M Suc-LLVY-amc containing 50 mM Tris-HCl pH 8.0 buffer solution and shaken at RT for 60 min in darkness. The gel was transilluminated at 360 nm using a Gel Logic 2200 gel imager (Carestream). For salinosporamide inhibition, proteasome was incubated with 75  $\mu$ M salinosporamide A for 20 min prior to loading of the gel.

**Denaturing Gel Analysis.** Protein samples were prepared for denaturing PAGE by boiling for 5 min prior to loading 5–15  $\mu$ g proteasome onto the gel. Samples were loaded onto an Invitrogen NuPAGE 16% Tris-glycine SDS gel and run at 125 V for 3 h. Gels were washed and stained with Coomassie Brilliant Blue.

**Proteasome Assays.** All proteasome assays were performed at a final volume of 50  $\mu$ L in Greiner half-well microplates at 30 °C in 50 mM Tris-HCl pH 8.0, unless otherwise specified. Fluorescence was measured on a Spectramax M2 plate reader (Molecular Devices) with an excitation wavelength of 355 nm and an emission wavelength of 460 nm.

**Rates of Hydrolysis.** Purified proteasome complexes were assayed at three concentrations, each in triplicate. Enzyme concentrations assayed varied by proteasome complex from 5 to 60  $\mu$ g mL<sup>-1</sup> depending on activity. Substrate was added to 40  $\mu$ M. Change in fluorescence was monitored continuously, and the slope of the steady state portion of the curve was used to calculate the hydrolysis rate at that enzyme concentration. The average hydrolysis rate at each enzyme concentration was then plotted and a line was fit to obtain the hydrolysis rate per enzyme concentration.<sup>39</sup> Relative fluorescence units were converted to  $\mu$ M by comparison to a standard curve of 7-amino-4-methylcoumarin in 50 mM Tris-HCl pH 8.0.

**Proteasome Inhibition.** Proteasome complexes were incubated in serial dilutions of the proteasome inhibitors for 15 min at 30 °C. Enzyme concentration was adjusted between 1–3  $\mu$ g per reaction (20–60  $\mu$ g mL<sup>-1</sup>) to ensure adequate activity for measurement of inhibition. Amounts of proteasome added per reaction were 1.2  $\mu$ g  $\alpha/\beta_1$ , 1.3  $\mu$ g  $\alpha/\beta_1$  M45F, 1.0  $\mu$ g  $\alpha/\beta_1$  A49V, 3.0  $\mu$ g  $\alpha/\beta_1$  M45F/A49V, 1.7  $\mu$ g  $\alpha/\text{SalI}$ , and 2.9  $\mu$ g  $\alpha/\text{SalI}$  F45M. The  $\alpha/\text{SalI}$  V49A and  $\alpha/\text{SalI}$  F45M/V49A mutants were not tested due to lack of hydrolytic activity. Fluorogenic substrate was then added to 40  $\mu$ M, and the reaction was allowed to proceed for 30 min in darkness before fluorescence was measured. Maximum activity was set as proteasome in the absence of inhibitor, and minimum activity was set as fluorogenic substrate in the absence of proteasome. Measurements were performed in triplicate and averaged. IC<sub>50</sub> values were calculated from 4-parameter logistic curve fittings.<sup>39</sup>

**Time-Dependence of Inhibition.** Dilutions of salinosporamide A or B ranging from 0.5 to 100  $\mu$ M and 40  $\mu$ M Z-VKM-amc substrate (final concentrations) were warmed to 30 °C in a 96-well plate. Prewarmed  $\alpha/\beta_1$  or  $\alpha/\text{SalI}$  was then added at 20  $\mu$ g mL<sup>-1</sup> (27 nM, 14 active sites) final concentration, and fluorescence was measured every minute for 3.5 h at a constant temperature of 30 °C.

**Irreversibility of Inhibition.** To assess the reversibility of salinosporamide A inhibition on the  $\alpha/\beta_1$  and  $\alpha/\text{SalI}$  complexes, 300  $\mu$ L of

20  $\mu$ g mL<sup>-1</sup> enzyme in 50 mM Tris-HCl pH 8.0 buffer was incubated with 250  $\mu$ M salinosporamide A or an equivalent amount of DMSO for 1.5 h at 30 °C. Samples were buffer exchanged three times on Amicon Ultra 0.5 mL 30 kDa cutoff centrifugal filters (Millipore) to remove inhibitor and added to a microplate containing 40  $\mu$ M Z-VKM-amc substrate. Fluorescence was monitored at 30 °C every minute for 3 h.

**Cinnabaramide Biosynthetic Gene Cluster Cloning.** DNA isolation and manipulations in *E. coli* and *Streptomyces* sp. JS360 were carried out according to standard methods.<sup>40,41</sup> PCR amplifications were carried out using Taq DNA polymerase (Fermentas). Fosmid sequencing was conducted by GenoTech Corp. A genomic fosmid library of *Streptomyces* sp. JS360 was constructed in pCC2 (Epicenter) according to manufacturer's protocol. This library was screened by colony PCR with degenerate ketosynthase primers based on five ketosynthase sequences: the tetronomycin synthase TetA from *Streptomyces* sp. NRRL 11266 (BAE93722), the tyactone synthase TylG from *Streptomyces fradiae* (O33954), the jamaicamide synthase JamE from *Lyngbya majuscula* (AAS98777), and the salinosporamide A and K synthase SalA and Sp\_SalA from *Salinospora tropica* (ABP73645) and *Salinospora pacifica* (ADZ28493), respectively. The primers were FP\_KSdeg 5' TGGGARGCDCTGGARGABGCBGGC 3', with a degeneracy of 108, and RP\_KSdeg 5' GCCGTYGGCDGCGGCGTCGAAGG 3', with a degeneracy of 6. The *cinJ* gene sequence was obtained through gene walking from the 5' end of the *cinA* polyketide synthase.

***Streptomyces* sp. JS360 Proteasome Gene Cloning.** The  $\alpha$ -subunit was cloned from *Streptomyces* sp. JS360 genomic DNA using the forward 5' GTGTGCGACGCCGTTCTATG 3' and reverse 5' GCTTG-AACTTGCCTGCTG 3' primers. Oligonucleotides were designed based on an alignment of  $\alpha$ -subunit genes from *Streptomyces scabiei* 87.22, *Streptomyces avermitilis* MA-4680, *Streptomyces coelicolor* A3,<sup>2</sup> *Streptomyces lividans* TK24, *Streptomyces griseus* NBRC 13350, and *Streptomyces ghanaensis* ATCC 14672. Specific primers were used subsequently to identify an appropriate fosmid, which was further used as template to obtain the primary proteasome  $\beta$ -subunit sequence through gene walking from the 5' end of the  $\alpha$ -subunit.

## ■ ASSOCIATED CONTENT

Supporting Information. This material is available free of charge via the Internet at <http://pubs.acs.org>.

## Accession Codes

The primary 20S proteasome  $\alpha$  and  $\beta$  subunit of *Streptomyces* sp. JS360 were deposited in GenBank with the accession number JF970179. The cinnabaramide associated 20S proteasome  $\beta$ -subunit was deposited in GenBank with the accession number JF970180.

## ■ AUTHOR INFORMATION

### Corresponding Author

\*E-mail: bsmoore@ucsd.edu.

## ■ ACKNOWLEDGMENT

This work was supported by a grant from the NIH (CA127622) to B.S.M. and the Albert and Anneliese Konanz Foundation, Mannheim, for a graduate fellowship to A.L.

## ■ REFERENCES

(1) Murata, S., Yashiroda, H., and Tanaka, K. (2009) Molecular mechanisms of proteasome assembly. *Nat. Rev. Mol. Cell Biol.* 10, 104–115.

- (2) Groll, M., Ditzel, L., Lowe, J., Stock, D., Bochtler, M., Bartunik, H. D., and Huber, R. (1997) Structure of 20S proteasome from yeast at 2.4 angstrom resolution. *Nature* 386, 463–471.
- (3) Borissenko, L., and Groll, M. (2007) 20S proteasome and its inhibitors: crystallographic knowledge for drug development. *Chem. Rev.* 107, 687–717.
- (4) Bross, P. F., Kane, R., Farrell, A. T., Abraham, S., Benson, K., Brower, M. E., Bradley, S., Gobburu, J. V., Goheer, A., Lee, S. L., Leighton, J., Liang, C. Y., Lostritto, R. T., McGuinn, W. D., Morse, D. E., Rahman, A., Rosario, L. A., Verbois, S. L., Williams, G., Wang, Y. C., and Pazdur, R. (2004) Approval summary for bortezomib for injection in the treatment of multiple myeloma. *Clin. Cancer Res.* 10, 3954–3964.
- (5) Groll, M., Berkers, C. R., Ploegh, H. L., and Ovaas, H. (2006) Crystal structure of the boronic acid-based proteasome inhibitor bortezomib in complex with the yeast 20S proteasome. *Structure* 14, 451–456.
- (6) Chauhan, D., Li, G. L., Shringarpure, R., Podar, K., Ohtake, Y., Hideshima, T., and Anderson, K. C. (2003) Blockade of Hsp27 overcomes bortezomib/proteasome inhibitor PS-341 resistance in lymphoma cells. *Cancer Res.* 63, 6174–6177.
- (7) Oerlemans, R., Franke, N. E., Assaraf, Y. G., Cloos, J., van Zantwijk, L., Berkers, C. R., Scheffer, G. L., Debipersad, K., Vojtekova, K., Lemos, C., van der Heijden, J. W., Ylstra, B., Peters, G. J., Kaspers, G. L., Dijkmans, B. A. C., Scheper, R. J., and Jansen, G. (2008) Molecular basis of bortezomib resistance: proteasome subunit  $\beta 5$  (PSMB5) gene mutation and overexpression of PSMB5 protein. *Blood* 112, 2489–2499.
- (8) Lu, S. Q., Yang, J. M., Song, X. M., Gong, S. L., Zhou, H., Guo, L. P., Song, N. X., Bao, X. C., Chen, P. P., and Wang, J. M. (2008) Point mutation of the proteasome  $\beta 5$  subunit gene is an important mechanism of bortezomib resistance in bortezomib-selected variants of Jurkat T cell lymphoblastic lymphoma/leukemia line. *J. Pharmacol. Exp. Ther.* 326, 423–431.
- (9) Ri, M., Iida, S., Nakashima, T., Miyazaki, H., Mori, F., Ito, A., Inagaki, A., Kusumoto, S., Ishida, T., Komatsu, H., Shiotsu, Y., and Ueda, R. (2010) Bortezomib-resistant myeloma cell lines: a role for mutated PSMB5 in preventing the accumulation of unfolded proteins and fatal ER stress. *Leukemia* 24, 1506–1512.
- (10) Gulder, T. A. M., and Moore, B. S. (2010) Salinosporamide natural products: potent 20S proteasome inhibitors as promising cancer chemotherapeutics. *Angew. Chem., Int. Ed.* 49, 9346–9367.
- (11) Hochstrasser, M. (1995) Ubiquitin, proteasomes, and the regulation of intracellular protein degradation. *Curr. Opin. Cell Biol.* 7, 215–223.
- (12) Knipfer, N., and Shrader, T. E. (1997) Inactivation of the 20S proteasome in *Mycobacterium smegmatis*. *Mol. Microbiol.* 25, 375–383.
- (13) Hong, B., Wang, L. F., Lammertyn, E., Geukens, N., Van Mellaert, L., Li, Y., and Anne, J. (2005) Inactivation of the 20S proteasome in *Streptomyces lividans* and its influence on the production of heterologous proteins. *Microbiology* 151, 3137–3145.
- (14) Darwin, K. H., Ehrst, S., Gutierrez-Ramos, J. C., Weich, N., and Nathan, C. F. (2003) The proteasome of *Mycobacterium tuberculosis* is required for resistance to nitric oxide. *Science* 302, 1963–1966.
- (15) Pearce, M. J., Mintseris, J., Ferreyra, J., Gygi, S. P., and Darwin, K. H. (2008) Ubiquitin-like protein involved in the proteasome pathway of *Mycobacterium tuberculosis*. *Science* 322, 1104–1107.
- (16) Festa, R. A., McAllister, F., Pearce, M. J., Mintseris, J., Burns, K. E., Gygi, S. P., and Darwin, K. H. (2010) Prokaryotic ubiquitin-like protein (Pup) proteome of *Mycobacterium tuberculosis*. *PLoS One* 5, e8589.
- (17) Watrous, J., Burns, K., Liu, W. T., Patel, A., Hook, V., Bafna, V., Barry, C. E., Bark, S., and Dorrestein, P. C. (2010) Expansion of the mycobacterial “PUPylome”. *Mol. Biosyst.* 6, 376–385.
- (18) Poulsen, C., Akhter, Y., Jeon, A. H.-W., Schmitt-Ulms, G., Meyer, H. E., Stefanski, A., Stuhler, K., Wilmanns, M., and Song, Y.-H. (2010) Proteome-wide identification of mycobacterial pupylation targets. *Mol. Syst. Biol.* 6, 386.
- (19) Moore, B. S., Eustáquio, A. S., and McGlinchey, R. P. (2008) Advances in and applications of proteasome inhibitors. *Curr. Opin. Chem. Biol.* 12, 434–440.
- (20) Udwarý, D. W., Zeigler, L., Asolkar, R. N., Singan, V., Lapidus, A., Fenical, W., Jensen, P. R., and Moore, B. S. (2007) Genome sequencing reveals complex secondary metabolome in the marine actinomycete *Salinispora tropica*. *Proc. Natl. Acad. Sci. U.S.A.* 104, 10376–10381.
- (21) Eustáquio, A. S., McGlinchey, R. P., Liu, Y., Hazzard, C., Beer, L. L., Florova, G., Alhamadsheh, M. M., Lechner, A., Kale, A. J., Kobayashi, Y., Reynolds, K. A., and Moore, B. S. (2009) Biosynthesis of the salinosporamide A polyketide synthase substrate chloroethylmalonyl-coenzyme A from S-adenosyl-L-methionine. *Proc. Natl. Acad. Sci. U.S.A.* 106, 12295–12300.
- (22) Hopwood, D. A. (2007) How do antibiotic-producing bacteria ensure their self-resistance before antibiotic biosynthesis incapacitates them? *Mol. Microbiol.* 63, 937–940.
- (23) Pouch, M. N., Cournoyer, B., and Baumeister, W. (2000) Characterization of the 20S proteasome from the actinomycete *Frankia*. *Mol. Microbiol.* 35, 368–377.
- (24) Nagy, I., Tamura, T., Vanderleyden, J., Baumeister, W., and De Mot, R. (1998) The 20S proteasome of *Streptomyces coelicolor*. *J. Bacteriol.* 180, 5448–5453.
- (25) Tamura, T., Nagy, I., Lupas, A., Lottspeich, F., Cejka, Z., Schoofs, G., Tanaka, K., Demot, R., and Baumeister, W. (1995) The characterization of a eubacterial proteasome: the 20S complex of *Rhodococcus*. *Curr. Biol.* 5, 766–774.
- (26) Zuhl, F., Tamura, T., Dolenc, I., Cejka, Z., Nagy, I., DeMot, R., and Baumeister, W. (1997) Subunit topology of the *Rhodococcus* proteasome. *FEBS Lett.* 400, 83–90.
- (27) Groll, M., Huber, R., and Potts, B. C. M. (2006) Crystal structures of salinosporamide A (NPI-0052) and B (NPI-0047) in complex with the 20S proteasome reveal important consequences of  $\beta$ -lactone ring opening and a mechanism for irreversible binding. *J. Am. Chem. Soc.* 128, 5136–5141.
- (28) Richter-Ruoff, B., Heinemeyer, W., and Wolf, D. H. (1992) The proteasome/multicatalytic-multifunctional proteinase. *In vivo* function in the ubiquitin-dependent N-end rule pathway of protein degradation in eukaryotes. *FEBS Lett.* 302, 192–196.
- (29) Sirikantaramas, S., Yamazaki, M., and Saito, K. (2008) Mutations in topoisomerase I as a self-resistance mechanism coevolved with the production of the anticancer alkaloid camptothecin in plants. *Proc. Natl. Acad. Sci. U.S.A.* 105, 6782–6786.
- (30) Puri, S. C., Verma, V., Amna, T., Qazi, G. N., and Spittler, M. (2005) An endophytic fungus from *Nothapodytes foetida* that produces camptothecin. *J. Nat. Prod.* 68, 1717–1719.
- (31) Nett, M., Guider, T. A. M., Kale, A. J., Hughes, C. C., and Moore, B. S. (2009) Function-oriented biosynthesis of  $\beta$ -lactone proteasome inhibitors in *Salinispora tropica*. *J. Med. Chem.* 52, 6163–6167.
- (32) Eustáquio, A. S., Nam, S. J., Penn, K., Lechner, A., Wilson, M. C., Fenical, W., Jensen, P. R., and Moore, B. S. (2011) The discovery of salinosporamide K from the marine bacterium “*Salinispora pacifica*” by genome mining gives insight into pathway evolution. *ChemBioChem* 12, 61–64.
- (33) Stadler, M., Bitzer, J., Mayer-Bartschmid, A., Muller, H., Benet-Buchholz, J., Gantner, F., Tichy, H. V., Reinemer, P., and Bacon, K. B. (2007) Cinnabaramides A-G: analogues of lactacystin and salinosporamide from a terrestrial streptomycete. *J. Nat. Prod.* 70, 246–252.
- (34) Rachid, S., Huo, L. J., Herrmann, J., Stadler, M., Kopcke, B., Bitzer, J., and Muller, R. (2011) Mining the cinnabaramide biosynthetic pathway to generate novel proteasome inhibitors. *ChemBioChem* 12, 922–931.
- (35) Feling, R. H., Buchanan, G. O., Mincer, T. J., Kauffman, C. A., Jensen, P. R., and Fenical, W. (2003) Salinosporamide A: a highly cytotoxic proteasome inhibitor from a novel microbial source, a marine bacterium of the new genus *Salinispora*. *Angew. Chem., Int. Ed.* 42, 355–358.
- (36) McGlinchey, R. P., Nett, M., Eustáquio, A. S., Asolkar, R. N., Fenical, W., and Moore, B. S. (2008) Engineered biosynthesis of antiprotealide and other unnatural salinosporamide proteasome inhibitors. *J. Am. Chem. Soc.* 130, 7822–7823.

(37) Jez, J. M., Ferrer, J. L., Bowman, M. E., Dixon, R. A., and Noel, J. P. (2000) Dissection of malonyl-coenzyme A decarboxylation from polyketide formation in the reaction mechanism of a plant polyketide synthase. *Biochemistry* 39, 890–902.

(38) Studier, F. W. (2005) Protein production by auto-induction in high-density shaking cultures. *Protein Expression Purif.* 41, 207–234.

(39) SigmaPlot, v. 11.0, Systat Software, Inc., San Jose, CA.

(40) Sambrook, J., Russell, D. (2001) *Molecular Cloning: A Laboratory Manual*, 3 ed., Cold Spring Harbor Laboratory Press, Cold Spring Harbor, NY.

(41) Kieser, T., Bibb, M. J., Buttner, M. J., Chater, K. F., Hopwood, D. A. (2000) *Practical Streptomyces Genetics*, John Innes Centre, Norwich, United Kingdom.